Enhanced photoluminescence emission from XSO4:Eu2+ (X = Mg, Sr) microphosphors

ARTICLE *in* INDIAN JOURNAL OF PHYSICS · MARCH 2014

Impact Factor: 1.38 · DOI: 10.1007/s12648-013-0411-4

4 AUTHORS, INCLUDING:

Partha Pal
Indian School of Mines
11 PUBLICATIONS **70** CITATIONS
SEE PROFILE

Pankaj Baitha
Indian School of Mines
6 PUBLICATIONS **6** CITATIONS
SEE PROFILE

Nitu Borgohain
Birla Institute of Technology, Mesra
12 PUBLICATIONS **17** CITATIONS
SEE PROFILE

Indian J Phys (March 2014) 88(3):243–250
DOI 10.1007/s12648-013-0411-4

ORIGINAL PAPER

Enhanced photoluminescence emission from $XSO_4:Eu^{2+}$ (X = Mg, Sr) microphosphors

P P Pal*, P K Baitha, N Borgohain and J Manam

Department of Applied Physics, Indian School of Mines, Dhanbad 826004, Jharkhand, India

Received: 05 September 2013 / Accepted: 10 October 2013 / Published online: 9 November 2013

Abstract: Microcrystalline powder of pure and Eu^{2+} doped $MgSO_4$ and $SrSO_4$ samples were prepared by high temperature re-crystallization method. X-ray diffraction, Scanning electron microscopy, energy dispersive spectroscopy and Fourier transform infrared spectroscopy studies were used to investigate the structural properties of prepared samples. It was observed that, in both cases, undoped and Eu^{2+} doped samples had same crystal structure confirming that small amount of rare earth ion doping did not change the basic structure of crystal. For optical characterization, photoluminescence (PL) and diffuse reflectance spectra of these samples were analyzed. The diffuse reflectance analysis was used to study bandgap of $XSO_4:Eu^{2+}$ samples. Many fold enhancement of PL emission peak was observed in doped sample when compared with undoped sample. These high intense spectra may have many uses in optoelectronic display devices. The enhancement mechanism was discussed in this paper.

Keywords: Rare-earth; Photoluminescence; Sulphate; Recrystallization

PACS Nos.: 78.55.Hx; 78.20.-e

1. Introduction

The rare earth (RE) activated phosphors are of great interest because of their drastic improvement in luminescence properties [1–3]. RE ion doped phosphors have been used in different fields because the intra-shell transition between 4f shells of rare-earth ions give sharp and intense emission lines [4, 5]. Among the RE ions, Eu is very much interesting due to its valence fluctuation property. It can remain in both Eu^{3+} and Eu^{2+} states [6, 7]. It gives red emission in Eu^{3+} state, whereas Eu^{2+} is very effective for yellow or green emission [8]. In most cases, emission of RE ions is due to optical transition within f intra-shell [e.g. Tb^{3+} ($4f^8$), Gd^{3+} ($4f^7$) and Eu^{3+} ($4f^7$)] [9, 10]. Yamashita et al. [11] and Nambi et al. [12] worked on $CaSO_4$:Dy for its dosimetric applications. Yamashita et al. [13] has further studied photoluminescence (PL) of $MgSO_4$ and $SrSO_4$, taking Eu^{2+} as rare-earth dopant. Chunxiang et al. [14] have studied emission spectra of $MgSO_4$, taking Dy as rare-earth ion and Mn as co-activator. All these studies show that rare-earth doped sulphate has great applications as luminescent materials. But for real applications of these materials in optoelectronic devices, enhancement of PL emission by rare-earth ions is to be studied more. Manam et al. [8] have reported manifold enhancement of luminescence of barium sulphate due to Eu^{2+} doping. Due to this intensive blue emission, Eu doped metallic sulphate compounds are extensively applied to lighting, field emission displays (FED), cathode ray tubes (CRT), plasma display panels etc. [15–17]. In this paper, PL studies of Eu^{2+} doped $MgSO_4$ and $SrSO_4$ prepared through high temperature re-crystallization method have been reported. It has been observed that doping of Eu^{2+} impurities in $MgSO_4$ and $SrSO_4$ host lattices plays an important role on PL process and enhances the PL sensitivity.

2. Experimental details

Micro-crystalline powder of pure and Eu activated XSO_4 (X = Mg and Sr) were prepared by high temperature re-crystallization method [18–20]. In this method 2 gm analytical reagent grade MCO_3 by weight 2 g was taken in a quartz crucible and 1.0 wt% of $EuCl_3$ was added to it. This mixture was then dissolved in concentrated sulphuric acid

*Corresponding author, E-mail: phys.ppal@gmail.com

Table 1 XRD peak positions and corresponding *d* spacing of Eu^{2+} doped $MgSO_4$

Peak position (experimental)	Peak position (reference)	*d* spacing (experimental)	*d* spacing (reference)	(*h k l*)
20.734	20.700	4.28062	4.2857	0 2 0
25.703	25.225	3.46324	3.5277	1 1 1
34.465	34.380	2.60014	2.6063	1 1 2
37.131	36.681	2.41937	2.4480	1 3 0
38.189	37.917	2.35471	2.3710	2 0 0
39.514	39.398	2.27877	2.2852	2 1 0
50.890	50.506	1.79288	1.8056	0 4 2
59.858	59.720	1.54392	1.5471	2 4 1

Table 2 XRD peak positions and corresponding *d* spacing of Eu^{2+} doped $SrSO_4$

Peak position (experimental)	Peak position (reference)	*d* spacing (experimental)	*d* spacing (reference)	(*h k l*)
24.008	23.578	3.70368	3.7700	1 1 1
26.358	25.931	3.37854	3.4330	0 0 2
27.464	27.037	3.24504	3.2950	2 1 0
28.503	28.062	3.12906	3.1770	1 0 2
30.497	30.042	2.92885	2.9720	2 1 1
33.927	33.483	2.64017	2.6740	0 2 0
44.700	44.344	2.02527	2.0410	1 1 3
45.695	45.327	1.98387	1.9990	4 0 1
48.953	49.011	1.85919	1.8570	3 2 1

(H_2SO_4, 98 % conc.). H_2SO_4 was taken in such an amount that whole mixture would dissolve in it. The quartz crucible was kept at 750 °C for 30 min and then rapidly cooled to room temperature. The sample was then crushed and sieved to obtain fine mesh powder. The undoped sample was prepared by same method without adding $EuCl_3$. Proper protection was needed keeping in mind the adverse effect of H_2SO_4 on skin and lungs before performing this experiment.

Characterization of prepared pure and doped XSO_4 samples were carried out by XRD, FTIR, SEM studies, PL and UV-Vis. XRD was recorded at room temperature in a wide range of Bragg angle 2θ ($10° \leq 2\theta \leq 65°$) in Bruker D8 Focus X-ray diffractometer at a scanning rate of 2°/min. FTIR spectrum was taken in KBr pellet method and recorded in region 4,000–400 cm^{-1} in FTIR-Spectrum RX I (Perkin Elmer, Switzerland) Spectrophotometer. Scanning Electron Microscopic study was also done using JEOL JSM-6390LV SEM instrument. The PL studies were performed on Hitachi F-2500 fluorescence spectrophotometer. The reflectance studies were performed on 'PERKIN ELMER make lambda 35' UV-Vis-NIR spectrophotometer

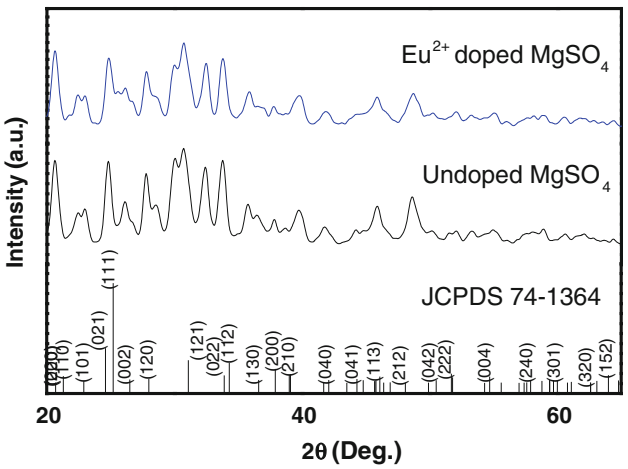

Fig. 1 XRD patterns for undoped and Eu^{2+} doped $MgSO_4$ along with JCPDS plot

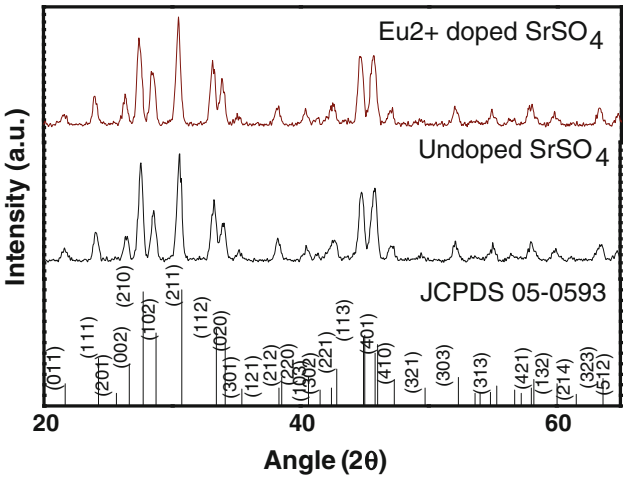

Fig. 2 XRD patterns for undoped and Eu^{2+} doped $SrSO_4$ along with JCPDS plot

respectively. The spectra were reported in terms of reflectance 'R' of the material where y-axis represents the fraction of incident light reflected at a given wavelength. These spectra were recorded in 200–700 nm range of wavelength.

3. Results and discussion

The room temperature XRD analysis carried out for undoped and europium doped XSO_4 (X = Mg, Sr) samples, are shown in Figs. 1 and 2, respectively to determine crystalline phase and lattice constant of samples. From analysis of XRD patterns, it is observed that peaks are sharp and single in both doped and undoped samples which suggesting no changes in phases occur due to doping. It is

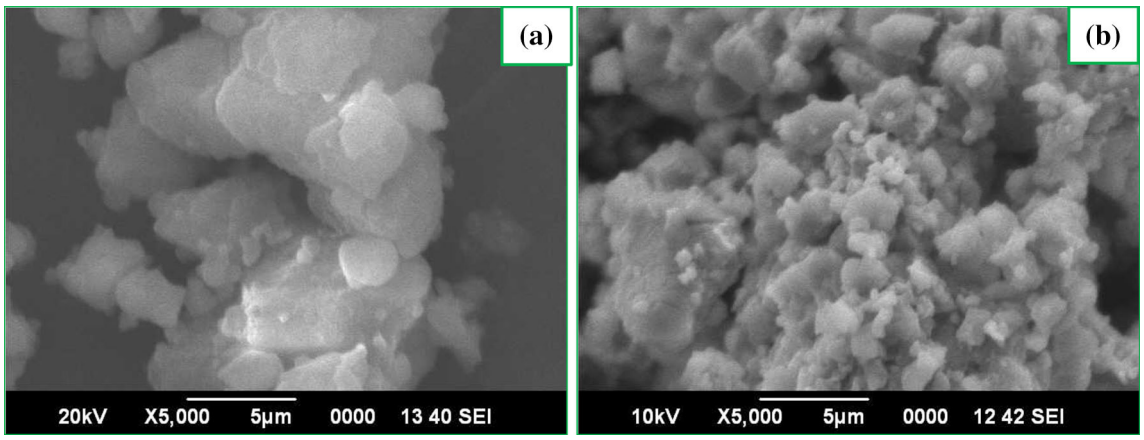

Fig. 3 SEM micrographs of (**a**) undoped and (**b**) Eu^{2+} doped $MgSO_4$

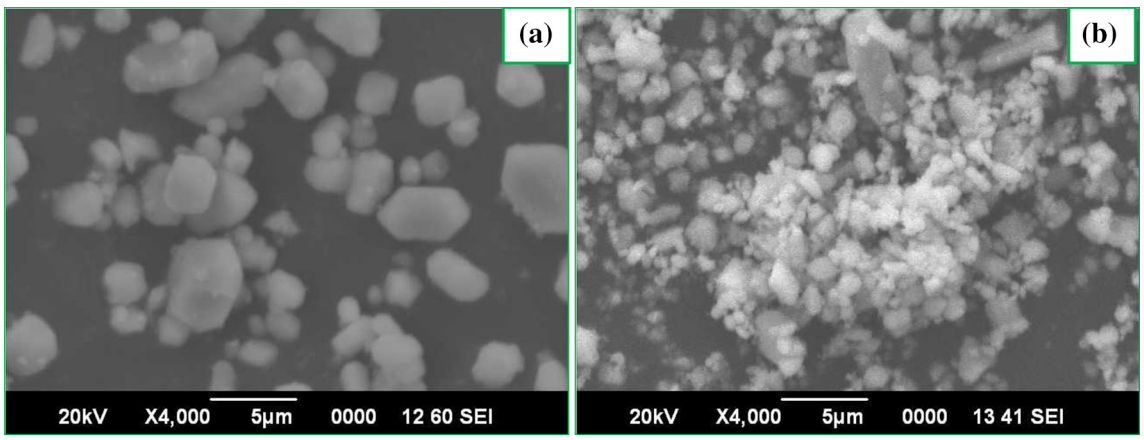

Fig. 4 SEM micrographs of (**a**) undoped and (**b**) Eu^{2+} doped $SrSO_4$

also found that prominent phases are $MgSO_4$ and $SrSO_4$. No change in XRD peak pattern is found in doped sample from undoped one due to very small doping amount of rare-earth. The wide range of XRD spectrum has a characteristic orthorhombic structure of a primitive lattice, where the lattice parameters for $MgSO_4$:Eu^{2+} and $SrSO_4$:Eu^{2+} are $a = 4.742$, $b = 8.575$, $c = 6.699$ and $a = 8.359$, $b = 5.352$, $c = 6.866$ respectively with $\alpha = \beta = \gamma = 90°$. All values are in correspondence with JCPDS card no. 74-1364 and 05-0593 for $MgSO_4$ and $SrSO_4$ respectively. From XRD pattern, inter planar spacing d have been calculated which shows a good agreement with respective JCPDS card. This result suggests suitability of crystal structure and unit cell parameter. (h k l) values of most prominent peaks for Eu^{2+} doped $MgSO_4$ and Eu^{2+} doped $SrSO_4$ and their corresponding d values are shown in Tables 1 and 2 respectively.

Morphology of micro structured undoped and Eu^{2+} doped XSO_4 samples have been studied by SEM images shown in Figs. 3(a), 3(b) and 4(a), 4(b) respectively. Single morphology is observed in both samples in SEM photograph. In case of Eu^{2+} doped $MgSO_4$, particle sizes are found to be in the range of 2–4 μm whereas, in case of Eu^{2+} doped $SrSO_4$, particles sizes are in the range 1–3 μm. This non-uniform distribution of particles sizes is caused due to non-uniform distribution of temperature and mass flow during the synthesis process [8]. The luminescence efficiencies largely depend on crystal size, particle morphology and particle sizes of the phosphor [21]. It is well known that efficiency of emission is optimum in the particle size range of 1.0–10 μm. Thus the samples are found to be very much suitable for PL measurements.

Energy dispersive spectroscopy (EDS) has been studied to observe elements present in sample. EDS analysis of Eu^{2+} doped $MgSO_4$ is shown in Fig. 5(a) and 5(b), which indicates that sample is composed of Mg, S, and O with a small amount of Eu, whereas, in the undoped sample Eu is not available. Figure 6(a) and 6(b) shows EDS analysis of

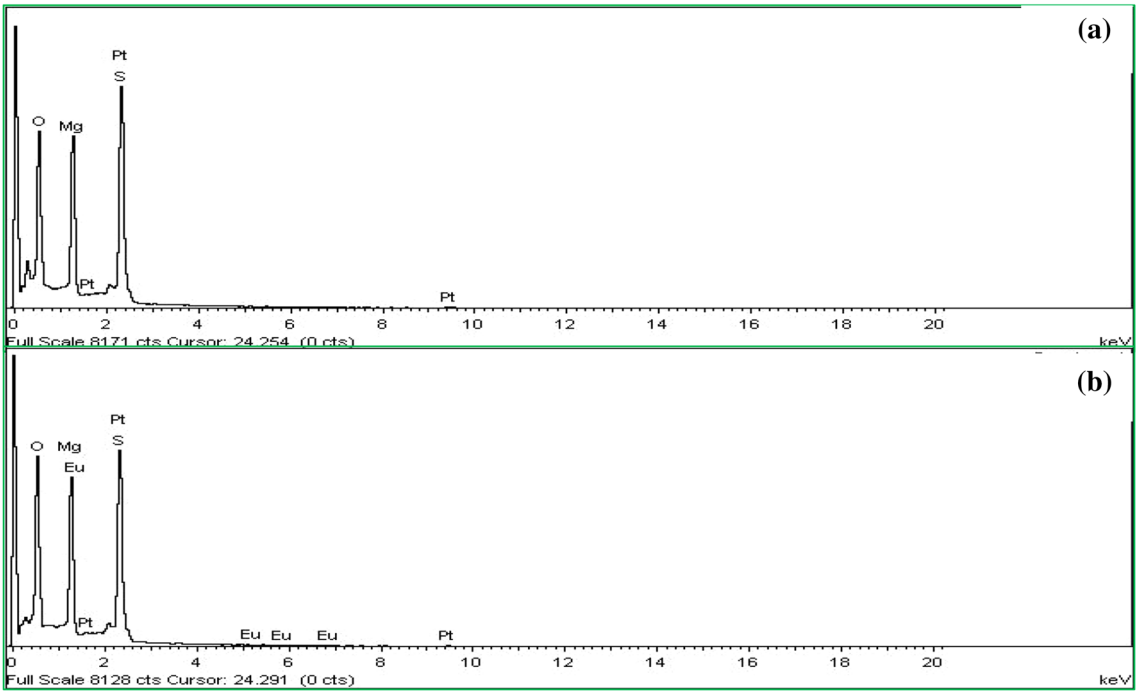

Fig. 5 EDS spectra of (**a**) undoped and (**b**) Eu^{2+} doped $MgSO_4$

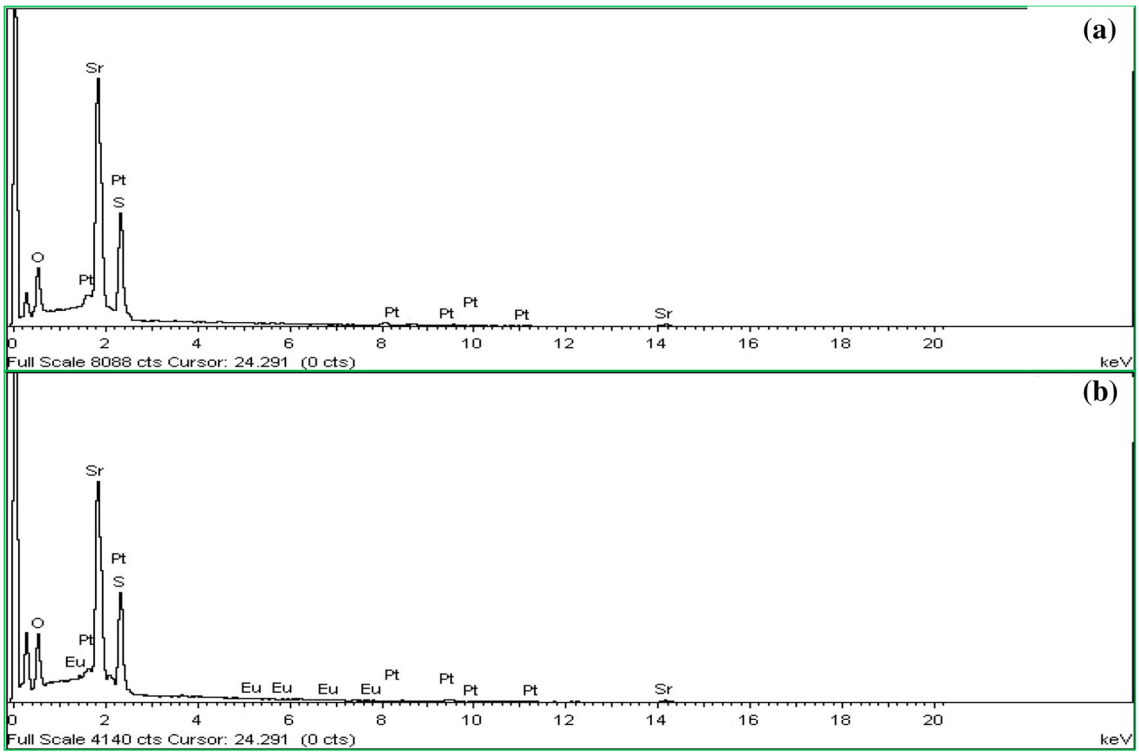

Fig. 6 EDS spectra of (**a**) undoped and (**b**) Eu^{2+} doped $SrSO_4$

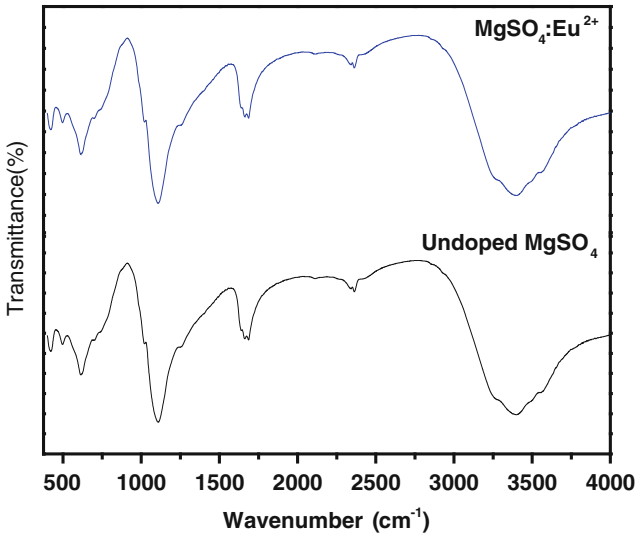

Fig. 7 FTIR spectra of undoped and Eu^{2+} doped $MgSO_4$

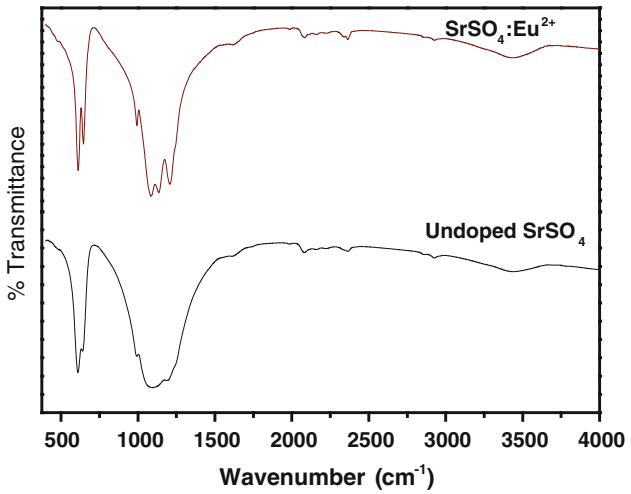

Fig. 8 FTIR spectra of undoped and Eu^{2+} doped $SrSO_4$

Eu^{2+} doped $SrSO_4$ indicating that sample is composed of Sr, S, O and Eu. EDS pattern confirms presence of europium in $MgSO_4$ and $SrSO_4$ powders and weight percentage of determined europium is very nearly equal to doped value of europium. Presence of Pt peak is observed due to Pt coating before characterization.

To confirm the formation of new Eu^{2+} doped $MgSO_4$ and $SrSO_4$ FTIR spectra of doped sample recorded in the range 400–4,000 cm^{-1}, are shown in Figs. 7 and 8. It has been reported that stretching band of sulphur and oxygen in inorganic compounds are found in the region 1,179–1,083 cm^{-1} [22, 23]. In our result, FTIR spectra of Eu^{2+} doped $MgSO_4$ and Eu^{2+} doped $SrSO_4$, sulphur oxygen stretch is found 1,023–1,112 and 1,087–1,207 cm^{-1} respectively. The band cantered at this region is due to

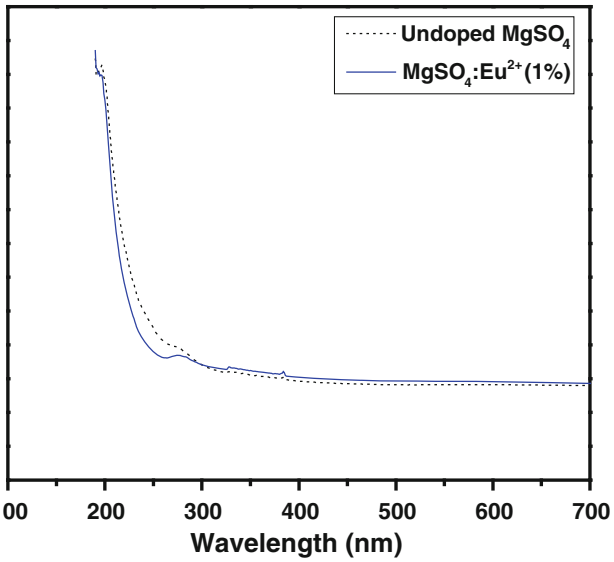

Fig. 9 Diffuse reflectance spectra of undoped and Eu^{2+} doped $MgSO_4$

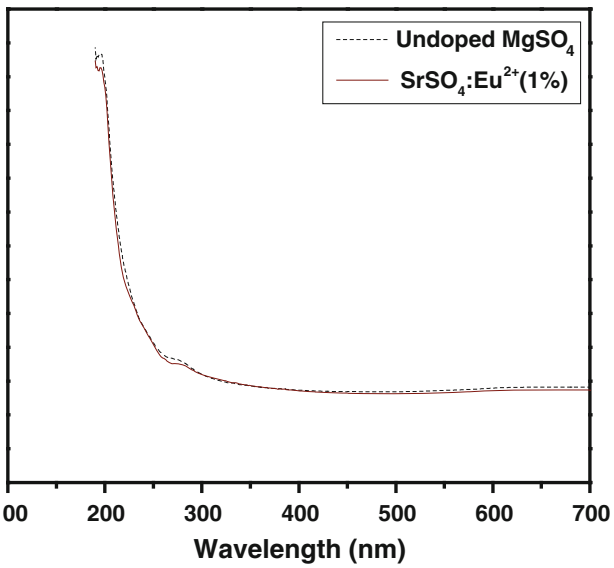

Fig. 10 Diffuse reflectance spectra of undoped and Eu^{2+} doped $SrSO_4$

symmetric vibration of SO_4^{2-} ion [24]. As suggested by Shen et al. [25], the peaks centered at 619 and 609 cm^{-1} in spectrum of doped $MgSO_4$ and $SrSO_4$ are due to out-of-plane bending vibration of SO_4^{2-}. It is well known that bending bands are sharper than stretching band in the inorganic infrared spectra which is clearly observed in the results obtained. Hence it can be concluded that metal sulfur bonds are formed in doped samples. It can also be interpreted that impurities are substitute for Sr ion without affecting co-ordinate environment around the central

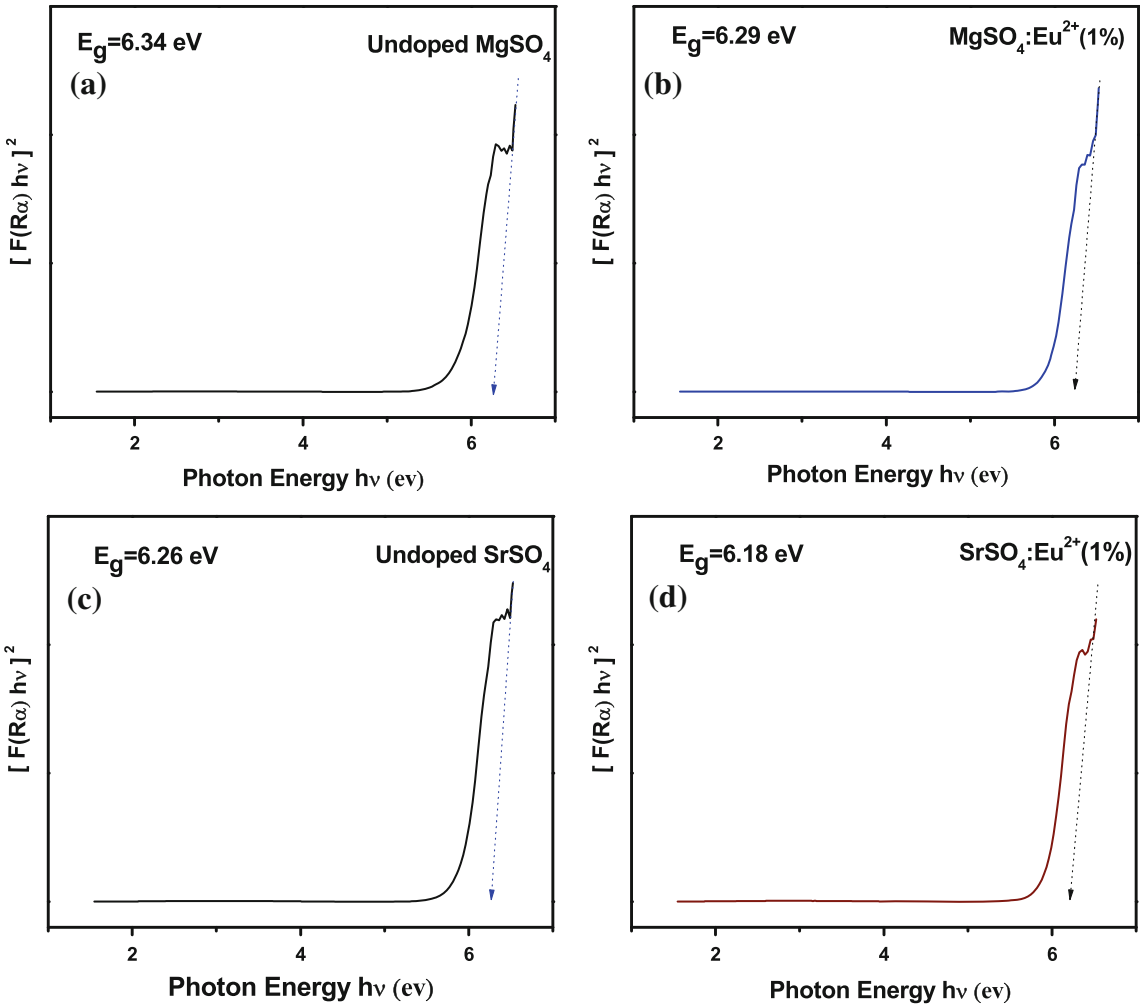

Fig. 11 Kubelka–Munk plots of (**a**) undoped $MgSO_4$, (**b**) $MgSO_4$:Eu^{2+}, (**c**) undoped $SrSO_4$ and (**d**) $SrSO_4$:Eu^{2+}

metal. The peaks near 2,000 cm^{-1} are overtones whereas absorption band appear near 1,600 and 3,000 cm^{-1}, which are due to atmospheric water vapors absorbed by KBr pallet.

The diffuse reflectance spectra of $MgSO_4$:Eu^{2+} and $SrSO_4$:Eu^{2+} phosphors are also studied. The reflectance spectra of undoped and Eu^{2+} doped $MgSO_4$ are shown in Fig. 9. From this figure, it is found that sample begins to absorb near 220 nm, which is consistent with its calculated energy gap value. Similarly, Fig. 10 shows reflectance spectra of undoped and Eu^{2+} doped $SrSO_4$ having similar patterns.

Bandgap of XSO_4:Eu^{2+} sample have been calculated from the diffuse reflectance study, from Kubelka–Munk relation to convert reflectance into a Kubelka–Munk function $F(R_\alpha)$, given by,

$$F(R_\alpha) = (1 - R_\alpha)^2 / 2R_\alpha \quad (1)$$

where R_α is reflectance of an infinitely thick sample with respect to a reference at each wavelength [26]. Kubelka–Munk function is a function equivalent to absorption coefficient. Bandgap energy of nanoparticles were calculated from slope of the graph where $[F(R_\alpha)hv]^2$ are plotted against photon energy hv. In Fig. 11(a)–11(d), band gap energy calculated for undoped and $MgSO_4$:Eu^{2+} samples are found to be 6.34 and 6.29 eV respectively whereas band gap energy calculated for undoped and $SrSO_4$:Eu^{2+} samples have been found to be 6.26 and 6.18 eV respectively. Bandgap is found to be decreased in case of Eu^{2+} doped XSO_4 samples. The decrease of band gap is mainly because for doping: shallow level donor impurities create energy levels in band gap near conduction band edge and shallow acceptor impurities create energy levels near valence band edge. With increase in amount of doping, density of state of these dopants increases and forms a continuum of states just like in bands and effectively decreasing bandgap [27, 28].

PL of samples $MgSO_4$:Eu^{2+} and $SrSO_4$:Eu^{2+} phosphors have been recorded to find the role of RE element Eu^{2+} incorporation in host lattice of $MgSO_4$ and $SrSO_4$

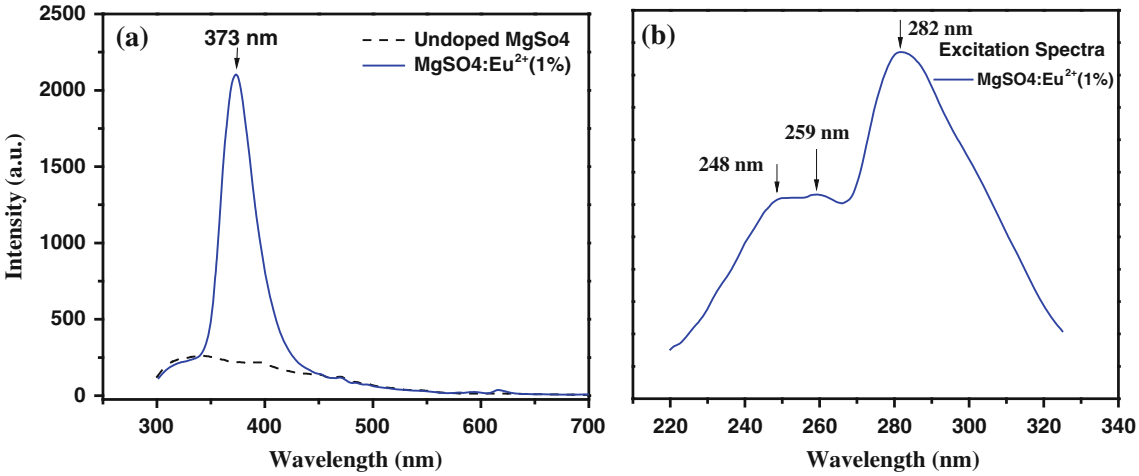

Fig. 12 Room temperature PL. (**a**) Emission and (**b**) excitation spectra of undoped and Eu^{2+} doped $MgSO_4$

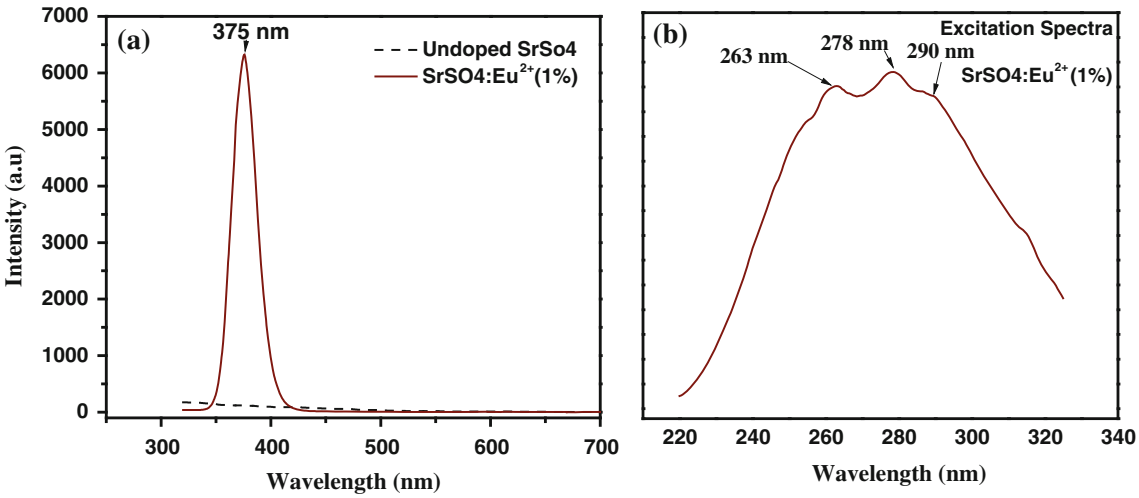

Fig. 13 Room temperature PL. (**a**) Emission and (**b**) excitation spectra of undoped and Eu^{2+} doped $SrSO_4$

respectively. Figure 12(a) and 12(b) shows PL emission and excitation spectra for doped and undoped $MgSO_4$, whereas, Fig. 13(a) and 13(b) shows the same for doped and undoped $SrSO_4$. PL emission spectra of $MgSO_4$:Eu^{2+}, at an excitation wavelength of 247 nm shows a single peak at 373 nm. This emission is due to $4f^6 5d \rightarrow 4f^7$ ($^8S_{7/2}$) transition of Eu^{2+} ions. The undoped sample shows a broadband from 300 nm to 400 nm which is found in relatively very less intensity than Eu^{2+} related peak. Eu^{2+} related peak is found to be almost 10 times more intense than host related peak. PL emission spectra of $SrSO_4$:Eu^{2+} phosphors, at an excitation wavelength 270 nm shows one peak at 375 nm, which is also characteristic emission of Eu^{2+} from lowest band of $4f^6 5d$–$^8S_{7/2}$ state of $4f^7$ configuration i.e. $4f^6 5d \rightarrow 4f^7$ ($^8S_{7/2}$) transition as shown in Fig. 13 [29, 30]. Eu^{2+} doping in $SrSO_4$ brings extraordinary enhancement in PL emission by increasing the intensity almost 25 times the emission for undoped sample. In simple words, the incorporation of europium ions by this recrystallization method increases this violet–blue emission several times, which shows that these materials (XSO_4) are excellent host materials for PL emission. To confirm the right selection of excitation wavelength, the room temperature PL excitation spectra of the samples are also investigated. It has been observed that the excitation spectra of $MgSO_4$:Eu^{2+} phosphor consists of three peaks at 248, 259 and 282 nm due to $4f^7 \rightarrow 4f^6 5d^1$ transitions [31, 32] of Eu^{2+} ion. Similarly, for $SrSO_4$:Eu^{2+}, three excitation peaks at 263, 278 and 290 nm corresponds to the typical $4f^7 \rightarrow 4f^6 5d^1$ transitions for the Eu^{2+} ion. These data confirms that high intense peaks caused by Eu^{2+} ions receive a suitable emission wavelength.

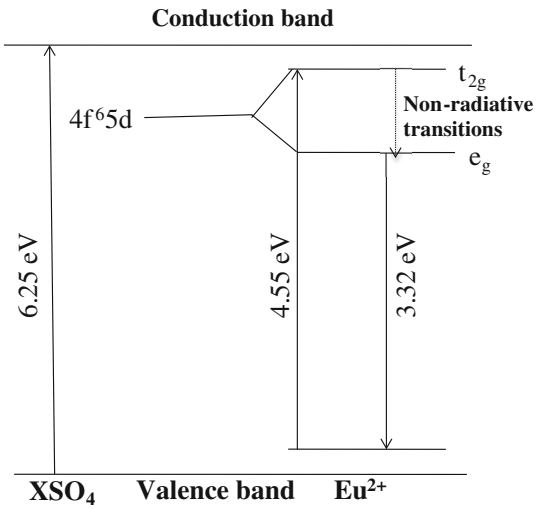

Fig. 14 Schematic energy levels of XSO_4:Eu^{2+} (X = Mg, Sr) samples

Figure 14 shows energy level diagram of Eu^{2+} doped XSO_4 (X = Mg, Sr) samples. Energy level can be realized in two different ways. First way is to excite Eu^{2+} ion directly in its own excitation levels. Electron from the ground state [$^4f_7$ ($^8S_{7/2}$)] of Eu^{2+} is excited into higher energy levels of Eu^{2+} [$^4f_6$5d (t_{2g})]. The excited free electron then relaxes to $^4f_6$5d (e_g) excited state of Eu^{2+} by a non-radiative process, followed by a radiative transition from $^4f_6$5d (e_g) excited state to $^4f_7$ ($^8S_{7/2}$) ground state, giving rise to typical emission of Eu^{2+} in XSO_4 host lattice. The second option is to excite host lattice, followed by efficient energy transfer from host lattice to Eu^{2+} ion, which also results in the typical emission of Eu^{2+}. Thus, PL emission and excitation spectra in doped sample are totally governed by transitions in Eu^{2+} ions.

4. Conclusions

XRD studies confirm that pure and Eu^{2+} doped $MgSO_4$ and $SrSO_4$ samples have orthorhombic structure at room temperature and particle size in the micrometer range was confirmed by SEM. The presence of Eu^{2+} in EDS pattern confirms formation of the doped $MgSO_4$ and $SrSO_4$ compounds. FTIR studies of doped and undoped samples performed at room temperature show that samples are free from any other organic functional group. The strong PL emission at about 373 and 375 nm of Eu^{2+} doped $MgSO_4$ and $SrSO_4$ respectively is consistence with their corresponding excitation spectra. The intensity of peak at 373 nm is found to be almost 10 times higher than that of host related peak for undoped $MgSO_4$, whereas, intensity of peak at 375 nm is found to be almost 25 times longer than that of host related peak for undoped $SrSO_4$.

Acknowledgments The authors are grateful to Dr. S.K. Sharma, Department of Applied Physics, Indian School of Mines, Dhanbad for valuable suggestions. P.P.P. and P.K.B. gratefully acknowledge funding by Indian School of Mines, Dhanbad.

References

[1] S Ekambaram and K C Patil *Bull. Mater. Sci.* **18** 7 (1995)
[2] P P Pal and J Manam *J. Rare Earths* **31** 37 (2013)
[3] P P Pal and J Manam *Mater. Sci. Eng. B* **178** 400 (2013)
[4] A Rukmangad, M Aynyas, S P Sanyal *Indian J. Phys.* **84** 1183 (2010)
[5] P P Pal and J Manam *Radiat. Phys. Chem.* **88** 7 (2013)
[6] Q Yanmin, Z Xinbo, Y Xiao, C Yan and G Hai *J. Rare Earths* **27** 2 (2009)
[7] H Yang et al. *J. Alloy Compd.* **454** 1 (2008)
[8] J Manam, P Kumari and S Das *Appl. Phys. A* **104** 197 (2011)
[9] C R Ronda, T Jüstel and H Nikol *J. Alloy Compd.* **275** 669 (1998)
[10] N V Chandra Shekar, V Kathirvel and P Ch Sahu *Indian J. Phys.* **84** 485 (2010)
[11] T Yamashita, N Nada, H Onishi and S Kitamura *Health Phys.* **21** 295 (1971)
[12] K S V Nambi, V N Bapat and A K Ganguly *J. Phys. C: Solid State Phys.* **7** 4403 (1974)
[13] N Yamashita, I Yamamoto, K Ninagawa, T Wada, Y Yamashita and Y Nakao *Jpn. J. Appl. Phys.* **24** 1174 (1985)
[14] Z Chunxiang, C Lixin, T Qiang, L Daling and Q Zhiren *Rad. Meas.* **35** 161 (2002)
[15] R P Yavetski, E F Dolzhenkova, A V Tolmachev, S V Parkhomenko, V N Baumer and A L Prosvirnin *J. Alloys Compd.* **441** 202 (2007)
[16] D S Thakare, S K Omanwar, P L Muthal, S M Dhopte, V K Kondawar and S V Moharil *Phys. Status Solidi A* **201** 574 (2004)
[17] K N Shinde, I M Nagpure, S J Dhoble, S V Godbole and M K Bhide *Indian J. Phys.* **83** 503 (2009)
[18] J Azorin, C Furetta and A Scacco *Phys. Status Solidi A* **138** 9 (1993)
[19] J Manam and S Das *J. Alloys Compd.* **489** 1 (2010)
[20] H H Adler and P F Kerr *Am. Miner.* **50** 132 (1965)
[21] X Qin and Y Jua *J. Mater. Res.* **20** 2960 (2005)
[22] B Smith *Infrared Spectral Interpretation: A Systematic Approach* (New York: CRC Press) p 95 (1999)
[23] K Nagamoto *Infrared Spectra of Inorganic and Coordination Compounds* (New York: Wiley Interscience) p 128 (1970)
[24] V Ramaswamy, R M Vimalathithan and V Ponnusamy *Adv. Appl. Sci.* Res. **1** 3 (2010)
[25] Y Shen, C Li, X Zhu, A Xie, L Qiu and J Zhu *J. Chem. Sci.* **119** 319 (2007)
[26] T Jia, W Wang, F Long, Z Fu, H Wang and Q Zhang *J. Alloys. Compd.* **484** 410 (2009)
[27] A Schenk *J. Appl. Phys.* **84** 3684 (1998)
[28] C V Vliet and P Vasilopoulos *Phys. Status Solidi* (*a*) **94** 635 1986
[29] R S Kher *Rad. Meas.* **46** 1372 (2011)
[30] A D Deshmukh, S J Dhoble, S V Godbole, M K Bhide and D R Peshwe *Indian J. Phys.* **83** 423 (2009)
[31] C Chartier, C Barthou, P Benalloul and J M Frigerio *J. Lumin.* **111** 147 (2005)
[32] T Matsuzawa, Y Aoki, N Takeuchi and Y Murayama *J. Electrochem. Soc.* 1**43** 2670 (1996)